Rock Mechanics 2, 189—204 (1970)
© by Springer-Verlag 1970

Determination of the Post-Failure Behavior of Brittle Rock Using a Servo-Controlled Testing Machine

By

F. Rummel* and **C. Fairhurst****

With 7 Figures

(Received April 27, 1970)

Summary — Zusammenfassung — Résumé

Determination of the Post-Failure Behavior of Brittle Rock Using a Servo-Controlled Testing Machine. The use of the servo-controlled testing machine to control fracture when a rock specimen is deformed beyond its peak strength is discussed. This region of deformation can not usually be examined because excess energy released by the loading system produces rapid disintegration of the specimen. In the test method described the energy release is controlled by a high frequency electronic servo-control system acting in combination with a hydraulic system of very short response time. The control causes the excess energy to be withdrawn before it can be released into the disintegrating specimen, by removing pressurized fluid from the hydraulic system.

Theoretical considerations reveal that the condition for controlled fracture is determined by the ability of the hydraulic loading system to unload rapidly. This may be expressed in terms of a 'dynamic stiffness', K_r, of the hydraulic system. For sufficiently small deformation rates and short servo-control response times the fracture process can be controlled, even though the unloading slope of the stress-strain curve of the rock specimen tends to become infinitely steep.

The experimental technique is described in detail and some results obtained in studying the post-failure behavior of Tennessee Marble under uni-axial and bi-axial compression using the new system are presented.

Bestimmung des Verhaltens von sprödem Gestein nach dem Bruch mittels eines servogesteuerten Prüfgerätes. Es wird über ein neues Verfahren berichtet, den Bruch spröden Gesteins zu kontrollieren, nachdem seine maximale Bruchlast überschritten ist. Dieser Bereich ist im allgemeinen der Untersuchung nicht zugänglich, da bei der Verwendung herkömmlicher Belastungs-Maschinen vom Belastungs-System ein Überschuß an Energie frei wird, der für eine explosionsartige Zerstörung des Gesteins verantwortlich ist. Bei dem hier beschriebenen Verfahren wird das Freiwerden der im System gespeicherten Energie durch ein hochfrequentes, elektronisch geregeltes Servo-System in Verbindung mit einer Hydraulik mit kurzer Verzögerungszeit kontrolliert. Es wird dabei der Gesteinsprobe zu jedem Zeitpunkt nur so viel Energie zugeführt wie zur Aufrechterhaltung für den stabilen Bruch notwendig ist.

Die theoretische Betrachtung des Systems zeigt, daß die Bedingung für den stabilen Bruch entlang der Post-Failure-Charakteristik durch die Fähigkeit des Belastungs-Systems bestimmt wird, rasch zu entladen. Der Begriff einer ‚dynamischen Steife' wird definiert.

* Post-doctoral Research Associate, School of Mineral and Metallurgical Engineering, University of Minnesota, Minneapolis, Minnesota 55455, U. S. A.

** Professor and Head, School of Mineral and Metallurgical Engineering, University of Minnesota, Minneapolis, Minnesota 55455, U. S. A.

Für genügend kleine Verformungsgeschwindigkeiten und kurze Verzögerungszeiten des Servo-Systems kann der Bruch auch dann kontrolliert werden, wenn die Neigung der Post-Failure-Kurve sich sehr großen Werten (— ∞) nähert.

Der Versuchsaufbau und die Versuchsdurchführung werden beschrieben und es werden einige Post-Failure-Kurven für Tennessee Kalkstein unter einachsiger und zweiachsiger Druckbeanspruchung wiedergegeben, wobei das neue Verfahren verwendet wurde.

•

Détermination du comportement après la rupture des roches fragiles au moyen d'une machine d'essai asservie. On présente un nouveau système pour contrôler la rupture des roches fragiles lorsque leur limite de rupture est dépassée. En général, il n'est pas possible d'étudier le comportement des roches dans ce domaine. L'emploi d'une machine d'essai traditionnelle libère inévitablement lorsque la limite de rupture est dépassée, un excès d'énergie qui provoque une violente désintégration de la roche. L'appareil, décrit dans cet article, contrôle la libération de l'énergie accumulée dans le système à l'aide d'un servo-système électronique à haute fréquence règlant un mécanisme hydraulique à temps de réponse très court. De cette facon, il est possible de limiter l'énergie transmise à la roche à la quantité nécessaire pour développer une rupture stable.

L'analyse théorique du système révèle que la possibilité d'obtention d'une rupture stable, la limite de rupture ayant été dépassée, est déterminée par la rapidité avec laquelle le système hydraulique peut se décharger. Le concept de rigidité dynamique est défini. Si les vitesses de déformation sont petites et si les temps de réponse du servosystème sont courts, il est possible de contrôler la rupture, même lorsque la pente du diagramme effort-déformation tend à devenir infiniment raide, la limite de rupture étant dépassée.

Le dispositif expérimental et l'exécution d'un essai sont décrits. Quelques diagrammes complets (y compris la partie descendante) d'un marbre du Tennessee pour les cas de compression simple et de compression double utilisant ce nouveau système sont présentés.

Introduction

Most rocks exhibit "brittle" behavior, failing violently and uncontrollably, when tested under unconfined conditions in conventional ("soft") hydraulic or screw-driven loading machines. It is now recognized that such rapid collapse is largely due to the design characteristics of the system used to load the specimen, and that it should be possible, under proper test conditions, to control the development of failure. Once this is achieved, the processes involved in disintegration can be studied in detail.

The violent collapse of a compressed specimen results from the rapid release of strain energy from the specimen-machine system after the maximum load bearing capacity (compressive "strength") of the rock specimen has been reached (Fig. 1). Control of the excess energy release rate should therefore lead to controlled deformation of the test specimen.

To date most attention has been given to the possibility of reducing energy stored in the loading system and available to act on the specimen, i. e., by increasing the rigidity of the testing frame. Considerable progress in studying the fracture processes in rock specimens and the physical properties of broken rock has been made through the use of such "stiff" testing machines. The high stiffness has been obtained in several ways — Turner and Barnard (1962) designed a system involving minimum fluid volume which was successfully used on concrete; Cook and Hojem (1966), Wawersik (1968) employed thermal contraction of the machine columns so as to gradually deform the specimen; in other cases the stiffness was increased by loading steel columns or steel rings in parallel with the rock specimen (Cook, 1965; Hughes and Chapman, 1966; Bieniawski, 1967, 1969). These experiments demonstrated that explosive failure of rock specimens, even under uni-axial stress, is not an intrinsic rock property. Wawersik, in the most comprehensive study reported to date, successfully developed for several rocks a controlled, continuous, progressive breakdown of the rock structure. He observed the sequence of macroscopic events which occur over the entire deformation range, from initial load application to complete disintegration of the material.

The above methods have been largely unsuccessful, however, in controlling the failure of hard rocks (fine-grained, high elastic modulus) particularly over the regions of deformation where the (negative) slope of the force-deformation locus exceeds the maximum attainable stiffness of the testing system.

Currently available servo-controlled loading systems have been generally considered unsuitable for controlling rock failure because of the finite response time of all servo-systems (Jaeger and Cook, 1969, p. 171). This paper presents

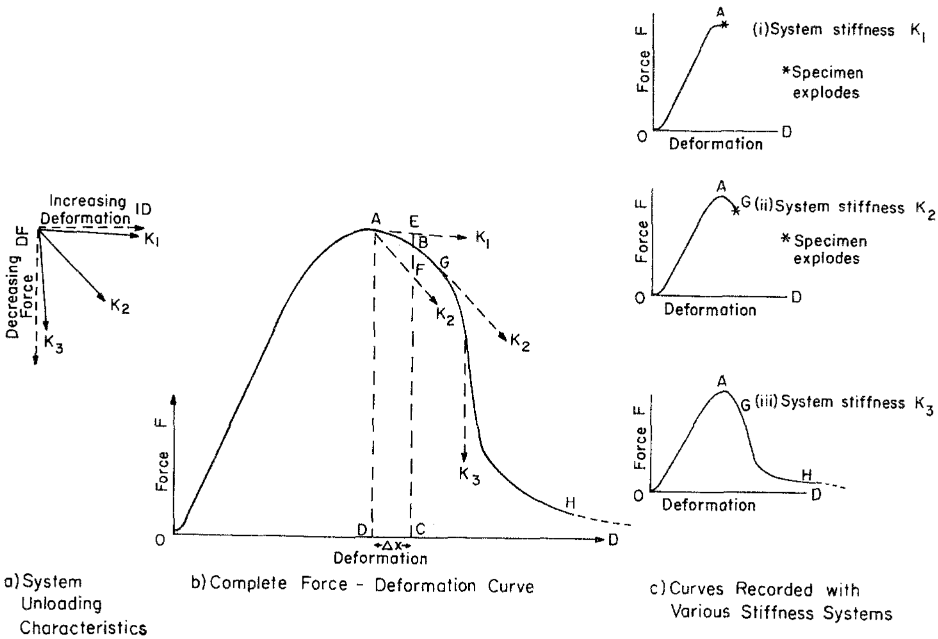

Fig. 1. Effect of system unloading stiffness on the recorded force-deformation behavior of a "brittle" material

Einfluß der Steifigkeit des Prüfgerätes auf das beobachtete Spannungs-Verformungs-Verhalten eines „spröden" Materials

K_1, K_2, K_3 Verlauf bei verschiedener Maschinensteifigkeit. F Kraft; D Verformung. a) Systemcharakteristiken bei Entlastung. ID zunehmende Verformung; DF abnehmende Kraft. b) Vollständiges Kraft-Verformungsdiagramm. c) Aufgezeichnete Diagramme bei verschiedener Systemsteifigkeit. *(i), (ii), (iii)* für Systemsteifigkeit K_1, K_2, K_3. * die Probe zerplatzt

Effet de la rigidité du système durant le déchargement effectué sur une matière fragile

K_1, K_2, K_3 différentes rigidités du système; D déformation. a) Caractéristiques du système de déchargement. ID déformation croissante; DF force décroissante. b) Courbe complète effort-déformation. c) Courbes enregistrées avec des systèmes ayant différentes rigidités. *(i), (ii), (iii)* rigidités K_1, K_2, K_3. * Explosion de l'échantillon

details of recent experiments using servo-control which indicate that this view is incorrect, at least for many rocks tested in compression, in that the response time appears to be adequate for control of the loading. A servo-controlled testing machine has been successfully used to determine the complete force deformation curve for specimens deformed in compression until totally disintegrated. Complete control of the deformation was possible even through the slope of the post-peak load region of the curve (i. e., deformation increasing, force decreasing) was very steep, approaching a vertical descent.

Influence of Testing System Stiffness on Observed Force-Deformation Behavior

The influence of the unloading stiffness of a testing system on the recorded force-deformation behavior can be illustrated by reference to Fig. 1.

The unloading stiffness, K, of the testing system may be defined as the ratio between the change (drop) in force, ΔF, applied by the loading platens, and the corresponding change in platen displacement Δx. Thus

$$K = \frac{\Delta F}{\Delta x} \tag{1}$$

and is generally negative, although (active)[1] systems can be arranged to give, effectively, a positive (i. e., decreasing deformation with decreasing force) unloading stiffness (Wawersik, 1968). Fig. 1 (a) illustrates three hypothetical stiffnesses, viz:

K_1 — representative of a "soft" testing system; approaching a "dead-weight" or constant force loading;

K_2 — representative of a stiffened system;

K_3 — representative of a very stiff system; approaching perfect rigidity or "fixed grips" loading.

We will assume that the complete applied-force versus deformation behavior for controlled deformation is as indicated by the curve $OABGH$ in Fig. 1 (b), and that it is not affected by the deformation rate. The slope of the tangent to the complete curve defines the (varying) rock specimen stiffness (K_r). If the specimen is deformed in a system of stiffness K_1, then as soon as point A (Fig. 1 b) is reached, i. e., the system starts to unload, the load exerted by the platens will follow the path AE, whereas the load that can be sustained by the specimen follows path AB. Thus, over the deformation Δx (equal to DC) the energy output of the system is represented by the area $AECD$ compared to the energy required for controlled deformation of the specimen, i. e., area $ABCD$. The excess energy, area AEB, accelerates the specimen deformation. Approximating the curve segment AB as a straight line of slope K_r, the excess energy (ΔW) released over the deformation increment given by Δx will be

$$\Delta W = \frac{(K_1 - K_r)\,(\Delta x)^2}{2}, \tag{2}$$

The energy imbalance increases rapidly with further deformation and the specimen disintegrates violently. Since most slow-speed recorders cannot accurately respond to very rapid signal changes, the intelligible portion of the force-deformation record appears somewhat as shown in Fig. 1 (c) (i). If the system stiffness is K_2 then the rock can be deformed in a controlled fashion over the region AB. Extra

[1] An 'active system' may here be defined as one where the unloading stiffness is determined by controls which are activated by the onset of unstable fracturing.

energy (e. g., fluid under pressure), equal to ABF must be introduced into the system to maintain the force at the values necessary to deform along AB. With this system the specimen can be deformed to point G, where K_2 becomes less steep than the local slope K_r and unstable, rapid deformation ensues. The recorded deformation will appear as in Fig. 1 (c) (ii) .

To control deformation over the complete range requires that the system stiffness be greater than that of the specimen for the steepest part of the unloading curve. This will be achieved for a sysem of stiffness K_3.

Use of Servo-Controls to Achieve High Effective Stiffness

Effective Unloading Stiffness of the Servo-Control System

As mentioned earlier, standard hydraulic loading systems are usually too soft to allow controlled deformation of the test specimen over the post peak-load region. The servo-control effectively increases the stiffness by extracting fluid from the pressurization system during the unloading deformation. In Fig. 1 (b), for example, the servo-controlled pump could be activated by a signal generated by the onset of instability at A. The effective fluid pressure would then be rapidly reduced such that instability did not develop further.

The action of the control may be explained by reference to Fig. 2, where F_0 may be taken to correspond to the force acting at the onset of instability; say point A in Fig. 1 (b).

It is important to note that this analysis assumes the time interval between the start of an unloading deformation and full-flow of the pump extracting the pressurized fluid to be negligibly small compared to the time during which the

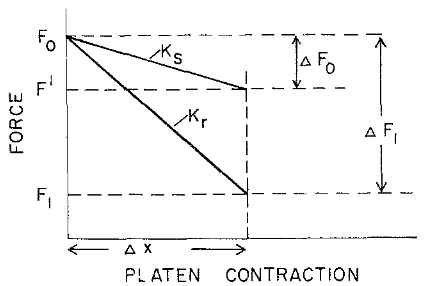

Fig. 2. Representation of effective stiffness of a servo-controlled system
K_s system unloading stiffness; K_r slope of the rock failure characteristic

Schematische Darstellung der effektiven Steifigkeit eines elektronisch geregelten Belastungssystems
F Kraft; K_s Maschinensteifigkeit; K_r Neigung der Verformungs-Belastungs-Kurve im Post-Failure-Bereich; ΔX Druckplattenverschiebung

Représentation de la rigidité effective d'un servosystème
K_s rigidité du système; K_r pente de la courbe caractéristique après la rupture de la roche; ΔX déformation

unloading deformation occurs, i. e., the "response-time" of the servo-system is small enough to consider it to react "instantaneously". The validity of this assumption will be discussed later. If no fluid is extracted from (or added to) the pressurized volume then a (small) platen contraction "Δx" will result in a fluid pressure drop Δp_0, corresponding to a drop ΔF_0 in platen force, i. e.,

$$\Delta F_0 = A \Delta p_0 \tag{3}$$

where A is the cross-sectional area of the pressurized cylinder used to drive the platen.

The unloading stiffness of the system K_s, is thus defined as

$$K_s = \frac{\Delta F_0}{\Delta x}. \tag{4}$$

If some of the fluid is withdrawn during the same platen deformation, Δx, then a greater pressure drop will occur, and the unloading stiffness will be effectively increased. To obtain an effective stiffness of K_r as shown in Fig. 2, it will be necessary to reduce the pressure by an amount Δp_1, where

$$\Delta F_1 = A \Delta p_1; \quad \text{and} \quad K_r = \frac{\Delta F_1}{\Delta x}. \tag{5}$$

The volume of fluid that must be extracted during the platen contraction Δx is readily calculated as follows:

Let "k" be the apparent bulk modulus (i. e., allowing for the dilatancy of the pressurization system components as well as that of the fluid itself) of the fluid system.

If no fluid is removed, the increase ΔV_0 in fluid volume due to the pressure drop Δp_0 (and platen contraction Δx) is, from the definition of bulk modulus,

$$\Delta V_0 = \frac{V_0 \cdot \Delta p_0}{k}. \tag{6}$$

Substituting from Eqs. (3) and (4), we obtain

$$\Delta V_0 = \frac{V_0 \cdot K_s \cdot \Delta x}{A k}. \tag{7}$$

If no fluid is removed, and the volume is allowed to expand until a drop in force of ΔF_1 takes place, then the fluid volume will increase by an amount of ΔV_1, where

$$\Delta V_1 = \frac{V_0 \cdot \Delta F_1}{A k}. \tag{8}$$

Substituting from Eq. (5) we obtain

$$\Delta V_1 = \frac{V_0 \cdot K_r \cdot \Delta x}{A k}. \tag{9}$$

Thus, the volume, ΔV^1, of fluid which must be removed in order to result in a force drop of ΔF_p for a platen contraction Δx (i. e., an effective stiffness of K_r) is

$$\Delta V^1 = \Delta V_1 - \Delta V_0. \tag{10}$$

From Eqs. (6) and (9), we obtain

$$\Delta V^1 = \frac{V_0 (K_r - K_s) \cdot \Delta x}{A k}. \tag{11}$$

Dividing both sides of Eq. (11) by the time interval, Δt, over which the platen displacement Δx occurs and recognizing that

$$\text{Limit}_{\Delta t \to 0} \frac{\Delta x}{\Delta t} = \dot{\varepsilon} L = \dot{\delta} \tag{12}$$

where

L is the height of the test specimen,

$\dot{\varepsilon}$ is the overall strain rate applied to the specimen,

$\dot{\delta}$ is the overall displacement rate between the ends of the specimen.

We may define the pumping rate, $\dot{Q}$, necessary to achieve an effective unloading stiffness, K_r, of a system deforming a specimen of length L at an overall strain rate, $\dot{\varepsilon}$. Thus,

$$\dot{Q} = \text{Limit}_{\Delta t \to 0} \frac{\Delta V^1}{\Delta t} = \frac{V_0 \cdot (K_r - K_s) \cdot \dot{\varepsilon} L}{A k}. \tag{13}$$

where $\dot{Q}$ is the rate at which the pressurized fluid must be extracted from the system to achieve an unloading stiffness of K_r.

Since, for a given experimental set up, all parameters in Eq. (13) except $\dot{\varepsilon} L = \dot{\delta}$ and $(K_r - K_s)$ are fixed the condition for controlled deformation along the post-failure locus may be written in the form

$$R = (K_r - K_s)\,\dot{\delta} \leqq \frac{k A}{V_0} \cdot \dot{Q}. \tag{14}$$

where the critical value of R defines the "rapid-unloading capability" of the hydraulic system at any instant. Thus, within the limits of deformation rates for which the servo response-time can be assumed negligibly small, the dynamic stiffness is, approximately, inversely proportional to the platen deformation rate selected.

If we assume K_s to be small compared to K_r, as appears to be true for rocks such as granites and hard limestones, then we may write Eq. (14) in the form

$$R = K_r\,\dot{\delta} \leqq \frac{k A}{V_0} \cdot \dot{Q}. \tag{15}$$

Servo-controlled deformation should therefore be possible as long as the unloading slope of the complete force-deformation curve does not exceed K_r given by Eq. (15).

Effect of Finite Response Time of the Servo-Controls

Actual servo-control systems do not, of course, respond instantaneously. A finite time, of the order of milliseconds, will elapse between detection of an instability in deformation (by the monitoring transducer) and adequate reduction of the applied force.

The sequence of events is illustrated in Fig. 3.

The specimen has been deformed, at a constant deformation rate $\dot{x}$ along the locus JK. At K, an instability starts to develop. Instantaneously, before the servo reacts, the system unloads as a fairly soft system, resulting in a rapid deformation along KL. At L the servo starts to act, causing the force to drop. The initial acceleration of the instability will be reduced but it will continue to deform, following a path such as LMN. Following Berry's (Berry, 1960) analysis of crack propagation, the instability has developed maximum kinetic energy at M, so that

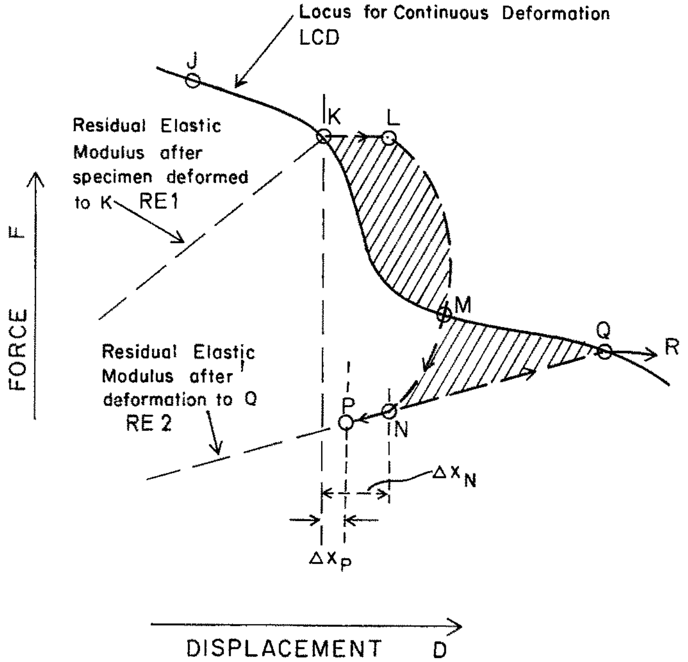

Fig 3. Idealized response of the servo-system to a rapidly generated instability

Vereinfachte Darstellung der Wirksamkeit eines Servosystems im Falle einer sich rasch ausbreitenden Instabilität im Post-Failure-Bereich

F Kraft; D Verschiebung; *JKMQ* Post-Failure-Kurve des Gesteins; *LCD* Bereich kontinuierlicher Verformung; *RE 1* Rest-Elastizitätsmodul nach Verformung der Probe bis K; *RE 2* Rest-Elastizitätsmodul nach Verformung bis Q

Réponse idéalisée d'un servo-système à une instabilité créée très rapidement

JKMQ courbe caractéristique de la post-fracture de la roche; *LCD* lieu de la déformation continue; *RE 1* module élastique résiduel après que l'échantillon ait été déformé jusqu'en K; *RE 2* module élastique résiduel après déformation jusju'en Q

the specimen continues to be deformed, "overshooting" the force corresponding to the critical value for slow deformation (i. e., the force at M). As the force drops, the instability decelerates and eventually halts at some state N. Assuming that the deformation from K to N has occurred in time "t", and the programmed constant deformation rate is $\dot{x}$, such that $\dot{x}t = \Delta x_p$, then the servo-system will command further unloading, since the specimen is over-deformed (to Δx_N), and this will now occur along the residual elastic curve, to point P, such that the deformation between K and P is Δx_p. Deformation will then continue at the programmed rate ($\dot{x}$), along the elastic path PNQ until the failure locus is reached at Q, and the cycle is repeated.

The above response of a servo-system will occur in a time of the order of tens of milliseconds. Unstable crack propagation in an ideally elastic material loaded in tension occurs at an average velocity of the order of 30 $\cong$ 40 percent of the velocity of sound in the medium. At such a rate a rock specimen failed in

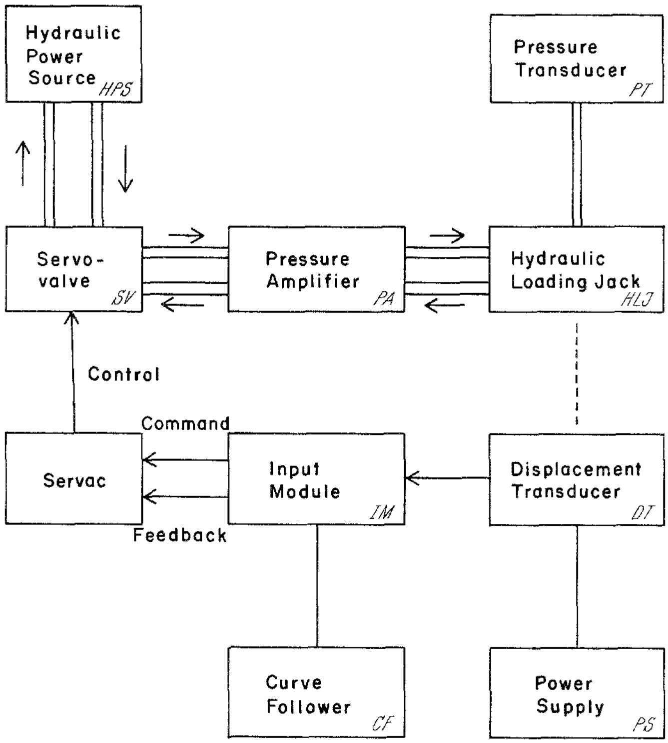

Fig. 4. Block diagram of the servo-controlled loading system

Schema eines servo-gesteuerten Belastungssystems

CF Diagramm-Abnehmer; *PS* Kraftversorgung; *DT* Verschiebungs-Steuerung; *IM* Eingangsmodul; *F* Rückkopplung; *SV* Servoventil; *HPS* hydraulische Kraftquelle; *PA* Druckverstärker; *HLJ* hydraulische Belastungspresse; *PT* Drucksteuerung

Diagramme schématique du système de chargement contrôlé par un servo-mécanisme

CF Suiveur de courbe; *PS* source de puissance; *DT* capteur de déplacement; *IM* boîte d'entrée; *HPS* source hydraulique de puissance; *PA* amplificateur de pression; *HLJ* vérin hydraulique; *PT* capteur de pression

direct tension should break into two parts within less than one-tenth of a millisecond from the time of crack initiation. While compressive collapse is probably more complex, similar rates may be predicted. A typical servo-system should therefore be incapable of arresting a potential instability.

The fact that such a system has been successful in controlling failure over the complete force-deformation range (see Fig. 5) strongly suggests that many rocks, when loaded close to failure, behave much differently than an ideal elastic material, at least for moderately slow strain rates, i. e., it appears that the instability develops much more slowly than would be predicted. There is substantial evidence to support the view that a regime of "slow" disintegration (or crack growth) precedes the onset of rapid failure in some materials (e. g., Vincent, 1962; Bieniawski, 1968).

Bieniawski, for example, has published results of measurements of crack velocities in rock specimens loaded in tension, and indicates slow crack growth (crack velocity less than 100 meters per second) until the crack had extended to

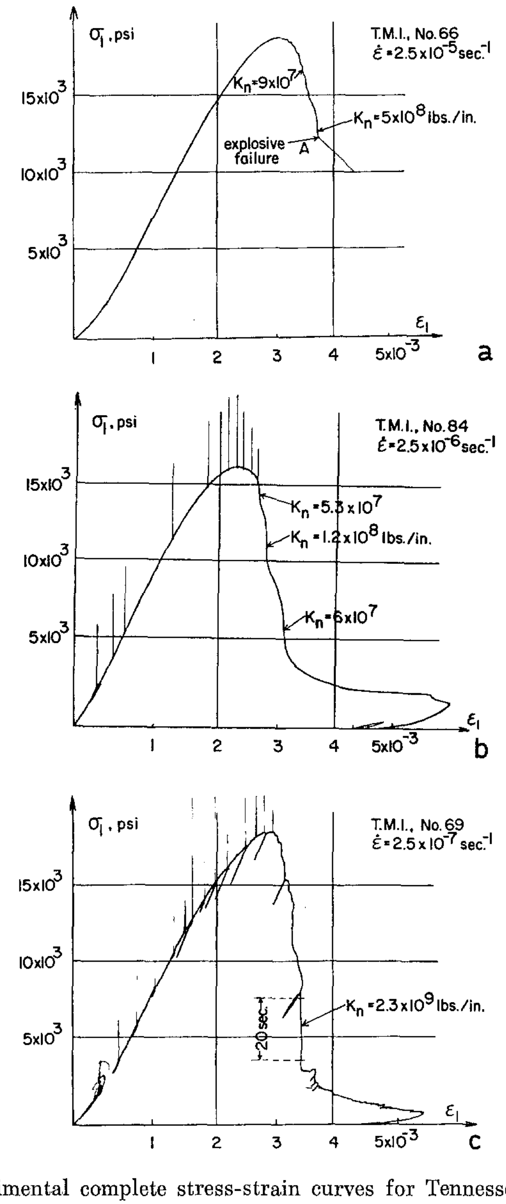

Fig. 5. Typical experimental complete stress-strain curves for Tennessee Marble at uni-axial compression and different constant strain-rates

Beispiele von vollständigen Spannungs-Verformungs-Kurven für Tennessee-Marmor unter einachsigem Druck und verschiedenen konstanten Verformungs-Geschwindigkeiten

Diagrammes expérimentaux complets d'essais en compression simple pour un marbre du Tennessee. Les diagrammes sont donnés pour plusieurs vitesses de déformation fifteen times its original length, beyond which it accelerated very rapidly to a high terminal velocity. This contrasts markedly with the theoretical behavior of an ideal elastic crack which reaches 50 percent of its (high) terminal velocity by the time it has doubled in length.

The development of non-linear behavior as the failure locus is approached along a path such as HK or NQ (Fig. 3) is evidence of (slow) rate-dependent deformation behavior just prior to the onset of major instability. These dissipative mechanisms will tend to be suppressed with increased deformation rates, so that rapid tests will be more difficult to conduct. Conversely, control should be easier under conditions which enhance energy dissipation mechanisms. Such conditions include high temperatures, compressive loading rather than tension, increased pressures, low strain rates, and heterogeneous rock structure.

The virtually continuous vertical drop in load observed in Fig. 5 is a noteworthy demonstration of the sensitivity of the control system.

Further studies of the "close-to-collapse" region of deformation are in progress. It is evident that changes such as slowly developing instability and rate-dependent energy dissipative mechanisms are operative in this region. A better understanding of these processes should also result in an improved explanation of related problems in rock failure.

Experimental Program

Two series of experiments were conducted. In one, unconfined cylindrical specimens were axially compressed to collapse; in the other the specimens were subjected to a constant, hydrostatic lateral confining pressure whilst being axially compressed.

Apparatus

The compression tests were carried out using Wawersik's (1968) loading frame, modified to allow servo-control of the applied load. The upper platen used to load the specimen was allowed to slide freely on the vertical columns, and the entire loading cycle was applied through a 100 ton, single acting hydraulic jack (EnerPac, Model SL 100). The hydraulic pressure was generated by an MTS Model 502-03 electric hydraulic power supply (3000 pounds per square inch cut-off), amplified by a 10 : 1 hydraulic pressure intensifier (Miller Fluid Company, Model H 72 BA 8).

The natural unloading stiffness of this system was found to be $8.6 \cdot 10^5$ pounds per inch.

The control circuit is shown in Fig. 4. The hydraulic pressure in the loading jack was controlled by means of a closed-loop electronic servo-system, which consisted of the servo-valve (Moog. ser. 73), the Servac (MTS, Model 401.03) and its input-module (MTS, Model 401.42), a displacement transducer and a Datatrak program commander for constant displacement-rate of the specimen (Fig. 4).

In the Servac-unit the command signal from the program commander, which represents the amount of desired displacement at time "t", is compared with the actual displacement of the specimen as measured by the displacement transducer (feed-back signal). The control signal of the Servac, which is proportional to the amount and direction of the error in displacement at time "t", causes the servo-valve to open in the direction required to compensate the error and by an amount proportional to the magnitude of the error. The electronic comparison is made at intervals of 10^{-4} seconds. The physical response time of the hydraulic system, which is mainly determined by the response time of the servo-valve, was measured as $5 \cdot 10^{-3}$ seconds. Because of the inertia of moving parts in the pressure amplifier and the loading jack, the time required to fully correct the displacement "error" varied between $10 \cdot 10^{-3}$ and $50 \cdot 10^{-3}$ seconds, depending on the magnitude of the error. All pressure tubing and connections were $^3/_8$ inch or larger in diameter. The maximum flow-capacity of the servo-valve at a pressure difference of 10^3 pounds per square inch between the two sides of the valve was 10 cubic inches per second. The program for constant displacement-rate (strain-rate) was plotted on a curve-following programmer (Data-trak, R. J. C., Model FGE 5110). Constant strain-rates between 10^{-4} and 10^{-8} were selected [based on the theoretical predictions of Eq. (14)]. The displacement was measured by a double-cantilever, strain gauge (full bridge) displacement indicator, the axial stress by a 6-inch-diameter by 5-inch-long mild steel strain gauge type load cell, and a 10,000 pounds per square inch capacity pressure transducer (BLH, Model GP-CG). Rando-HDA-oil (Texaco), was used as the low pressure fluid, with a light hydraulic oil (Standard Oil Company, No. 81) on the high pressure part of the system.

According to the experimental values of k, V_0, A and $\dot{Q}$ [$k = 10^5$ pounds per square inch, $V_0 \cong 10^2$ cubic inches, $A = 20$ square inches, $(\dot{Q})_{\max} = 10$ cubic inches per second) the critical value for $K_r \dot{\delta}$ in Eq. (15) was $2 \cdot 10^5$ pounds per second.

The pressure vessel used for the bi-axial compression tests is described by Wawersik (1968) and was designed for a maximum pressure of $15 \cdot 10^3$ pounds per square inch. The confining pressure was manually kept constant to within ± 1 pound per square inch by means of a high precision valve. The specimens were jacketed with a 2-inch-diameter irradiated polyolefin heat shrinkable tubing (Alpha Wire Company, Type FIT-221-2″).

The experiments were carried out on Tennessee Marble I (Wawersik, 1968). All specimens used were 4 inches long and 2 inches in diameter and were ground plane and parallel to within $\pm 0.5 \cdot 10^{-3}$ inch. A thin layer of powdered molybdenum disulphide was used to reduce the friction between the polished end-planes of the rock specimens and loading platen.

Results

Unconfined Tests

Complete stress-strain curves (derived from force-deformation curves) for Tennessee Marble I specimens loaded in unconfined compression, at three, different, constant strain-rates ($\dot{\varepsilon} = 2.5 \cdot 10^{-5}$; $2.5 \cdot 10^{-6}$; $2.5 \cdot 10^{-7}$ per second) are presented in Fig. 5. Because of the variation of the maximum compressive strength in the specimens of this particular rock, no significant strain-rate dependence of the strength could be noticed within the range of strain-rates employed. The influence of strain-rate on the onset and the amount of inelastic deformation during loading also appeared to be negligible for the strain-rates used. Time or strain-rate dependence of the deformation or fracture process, however, becomes significant in the descending portion of the complete stress-strain curve, where the average slope decreases with increasing strain-rate. This means that the decrease in load-carrying ability of the rock per unit of deformation at high strain-rates, is less than at lower strain-rates.

This result substantiates the previous comments concerning the rate-dependency of the inelastic deformation mechanisms. The probability for local fracture events is determined by fluctuation in the distribution of internal strain energy in time (Rummel, 1968).

According to the theoretical conclusions concerning the possibility for control [see comments following Eq. (15)], the maximum observable slope K_r in the post-failure region should not exceed the critical limit determined by substituting the actual values of k, V_0, A, $\dot{Q}$, and $\dot{\delta}$ into Eq. (15). (The unloading stiffness of the machine, K_s, may be neglected in comparison to K_r.) This yields the following values:

$\dot{\delta} = 10^{-4}$ inch per sec: $|K_r| = 9 \cdot 10^7 < 2 \cdot 10^9$ pounds per inch
$\dot{\delta} = 10^{-5}$ inch per sec: $|K_r| = 1.2 \cdot 10^8 < 2 \cdot 10^{10}$ pounds per inch
$\dot{\delta} = 10^{-6}$ inch per sec: $|K_r| = 2.3 \cdot 10^9 < 2 \cdot 10^{11}$ pounds per inch

Explosive failure occurred at point A in Fig. 5 (a) where, immediately before failure, K_r approached its critical value. To determine the values for K_r of the very steep portions of the post-failure curve, the values for $\dot{\delta}_r$ (or $\dot{\varepsilon}_r$) were taken from a force-time curve, plotted on an X-Y recorder with a time-base speed of 1 cm per second. Since all tests were performed at constant strain-rates, the time-axis in this case was equivalent to the strain-axis with high resolution.

The ability to control deformation with a system response time of 5 to 50 milliseconds substantiates the earlier comments to the effect that failure in Tennessee Marble, at least in compression, does not occur as rapidly as previously assumed. Potential deviations from the programmed deformation-rate are apparently corrected well before any appreciable instability can develop. It is concluded that the recorded complete stress-strain curves accurately describe the stress-conditions for progressive strain at constant strain-rate, independent of the deformation mechanisms acting.

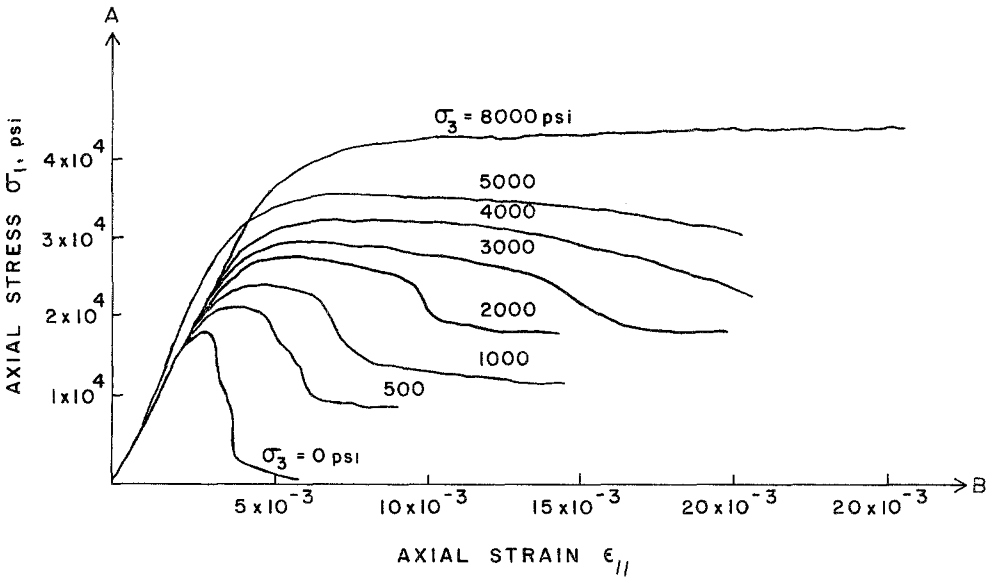

Fig. 6. Experimental stress-strain curves ($\sigma_1 - \varepsilon_1$) for Tennessee Marble at different confining pressures σ_3 and at constant strain-rate of 10^{-5} per second

Spannungs-Verformungs-Kurven (σ_1, ε_1) für Tennessee-Marmor bei verschiedenem konstanten Druck σ_3 und einer konstanten Verformungsgeschwindigkeit von 10^{-5} pro Sekunde
A axiale Spannung σ_1; B axiale Verformung ε_{11}

Diagrammes expérimentaux d'un marbre du Tennessee en compression double et à une vitesse déformation de 10^{-5} par seconde
A contrainte axiale; B déformation axiale

Similar results have also been obtained for various granites loaded in unconfined compression. More recently, the same control principles have been used successfully to control tension crack propagation in Ring and Brazilian tests on various rocks.

Partially loaded specimens were sectioned to determine the details of progressive damage. Essentially, the sequence of fracture events shown by Wawersik's experiments has been confirmed. Fracture becomes significant with the onset of local cracking, oriented predominantly parallel to the direction of the applied load; cracking begins at loads well before the maximum load bearing capability of the specimen is reached. This is indicated by the onset of rock noise activity (Scholz, 1968; Rummel, 1970), the onset of dilation (Crouch, 1970; Rummel, 1970) and the decrease of ultrasonic velocity perpendicular to the direction of loading (Rummel, 1970). The frequency and magnitude of local crack development increases rapidly with further deformation, particularly after the peak load is exceeded. This causes considerable structural damage as is indicated by the decrease in strength in the post failure region. A crack density of around 10^3 per square cm in the center section of a typical unconfined specimen was measured when it had been deformed to a point just before the development of inclined boundary fractures, cleavage slabs, and interior faults, which lead gradually to complete disintegration of the specimen. Some typical fracture patterns for different stages in the post-failure region are shown in Fig. 6.

Confined Tests

The bi-axial compression tests on Tennessee Marble I for different constant confining pressures up to 8000 psi were performed at a constant strain-rate of $2.5 \cdot 10^{-6}$ per second. The stress-strain curves presented in Fig. 7 represent the individual behavior of representative specimens. For confining pressures up to 2000 psi the local crack development with a predominantly axial orientation was progressively reduced and replaced by local shear failure, inter-crystalline gliding on inclined grain boundaries and intra-crystalline slip. Slabbing was prevented by only small confining pressures of several hundreds of pounds per square inch. The final

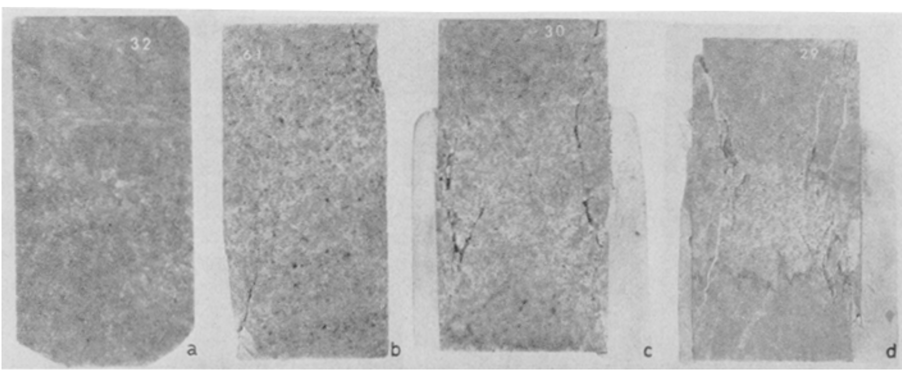

Fig. 7. Fracture patterns of unconfined specimens: a) at the peak of the stress-strain curve; b) after 30 % loss; c) after 50 % loss; d) after 70 % loss in load bearing capability

Rißverteilung in einachsig belasteten Proben von Tennessee-Marmor: a) belastet bis zur maximalen Bruchspannung; b) nach Überschreiten der Bruchspannung und bis zum Verlust von 30 %; c) von 50 %; d) von 70 % der maximalen Festigkeit

Vues de la rupture de la roche en compression simple. a) lorsque la limite de rupture est atteinte; b), c), d) lorsque 30, 50, 70 % de la capacité pertante est perdue macroscopic failure was still "brittle", up to confining pressures of 3000 pounds per square inch and is characterized in Fig. 7 by a relatively sudden decrease in the load-carrying capability of the specimens. Macroscopic failure for confining pressures $\sigma_3 = 2000$ pounds per square inch and $\sigma_3 = 3000$ pounds per square inch occurred always along a single shear plane. Stick-slip was not observed. For higher confinement the behavior of the rock beyond the maximum load became "quasi-plastic" in that no single macroscopic shear planes were developed within the range of applied deformation. At $\sigma_3 = 8000$ pounds per square inch the load-carrying capability of the rock gradually increased with increasing deformation. The stress-strain characteristic during this plastic stage of deformation is highly sensitive to the strain-rates employed.

Conclusion

Complete stress-strain curves have been obtained for various "brittle" rocks using a servo-controlled testing system. Analysis of the variables involved in the control operation indicates that deformations in the postpeak load (i. e., negative slope) region can be developed slowly and progressively by conducting the test at a sufficiently slow strain rate. Further, since the strain rate variable is controlled, a more objective experimental method is obtained. The form of the complete stress-strain curve was seen to be dependent on the applied strain rate.

Instability during rock disintegration appears to develop much more slowly than predicted by elastic theory. For rocks where this is true, deformation can be successfully controlled over the negative slope region, by a fast-acting servo-system. In such cases, the natural stiffness of the loading system becomes unimportant, so that it is not necessary to attempt to stiffen the frame unduly.

Closed-loop control appears to be of considerable utility in rock mechanics experiments where unstable situations are of interest. Crack propagation problems in particular can be studied in detail for a variety of situations.

Acknowledgements

The authors wish to acknowledge the valuable assistance and stimulating discussion by their colleagues John A. Hudson and Dr E. T. Brown, who are currently using the servo-control system. The research was made possible through the financial support of the American Petroleum Institute, the Petroleum Research Fund of the American Chemical Society, and the Advanced Research Project Agency.

References

Berry, J. P. (1960): Some Kinetic Considerations of the Griffith Criterion for Fracture. J. Mech. Phys. Solids, Vol. 8, 194–216.

Bieniawski, Z. T. (1967): Determination of Rock Properties. South African Council F. Sci. and Ind., Res. Rep., No. Meg 518.

Bieniawski, Z. T. (1968): The Phenomenon of Terminal Fracture Velocity in Rock. Reck Mech. and Eng. Geol., Vol. VI/3, 113–125.

Bieniawski, Z. T. (1969): Failure of Fractured Rock. Intern. J. of Rock Mech. Min. Sci., Vol. 6, 323–341.

Cook, N. G. W., and J. P. M. Hojem (Nov. 1966): A Rigid 50-Ton Compression and Tension Machine. South African Mec. Eng.

Cook, N. G. W. (1965): The Failure of Rock. Intern. J. Rock Mech. Min. Sci., Vol. 2, 4.

Crouch, S. L. (1970): Experimental Determination of Volumetric Strains in Failed Rock. In preparation.

Hughes, B. P., and G. P. Chapman (March 1966): The Complete Stress-Strain Curve for Concrete in Direct Tension. Bull. Rilem, No. 30.

Jaeger, J. C., and N. G. W. Cook (1969): Fundamentals of Rock Mechanics. London.

Rummel, F. (1969): Studies of Time-Dependent Deformation of Some Granite and Eclogite Rock Samples Under Uni-axial Constant Compressive Stress and Temperatures up to 400^0 C. Z. f. Geophys. *35,* 17–42.

Rummel, F. (1970): Determination of Rock Properties in the Post-Failure Region. In preparation.

Scholz, C. H. (1968): Microfracturing and the Inelastic Deformation of Rock in Compression. J. Geophys. Res., Vol. 73/4, 1417–1432.

Turner, P. W., and P. R. Barnard (1962): Stiff Constant Strain-Rate Testing Machine. Engineer *214,* 146–148.

Vincent, P. I. (1962): The Rupture Factor of Polymethylmetacrylate. British J. of Appl. Phys., Vol. 13, 578–582.

Wawersik, W. R. (1968): Detailed Analysis of Rock Failure in Laboratory Compression Tests. Ph. D. Thesis, University of Minnesota.

Addresses of the authors: Dr. F. Rummel, Institut für Geophysik der Ruhr-Universität Bochum, D-463 Bochum, Germany. Professor Charles Fairhurst, School of Mineral and Metallurgical Engineering, Institute of Technology, University of Minnesota, Minneapolis, Minnesota, U. S. A.